



A third-order weighted essentially non-oscillatory-flux limiter scheme for two-dimensional incompressible Navier-Stokes equations

Rooholah Abedian*

School of Engineering Science, College of Engineering, University of Tehran, Iran.

Abstract

In this paper, the 2D incompressible Navier-Stokes (INS) equations in terms of vorticity and stream function are considered. These equations describe the physics of many phenomena of scientific and engineering. By combining monotone upwind methods and weighted essentially non-oscillatory (WENO) procedures, a new numerical algorithm is proposed to approximate the solution of INS equations. To design this algorithm, after obtaining an optimal polynomial, it is rewritten as a convex combination of second-order modified ENO polynomials. Following the methodology of the traditional WENO procedure, the new non-linear weights are calculated. The performance of the new scheme on a number of numerical examples is illustrated.

Keywords. Navier-Stokes equation, WENO, UNO limiter.

2010 Mathematics Subject Classification. 35Q30, 35L99, 65M06.

1. INTRODUCTION

The INS equations

$$\mathbf{u}_t + (\mathbf{u} \cdot \nabla)\mathbf{u} + \nabla p = \varepsilon \Delta \mathbf{u}, \quad (1.1)$$

where p , $\mathbf{u} = (\tilde{u}, \tilde{v})^T$ and ε are the pressure, the divergence-free velocity field satisfying $\tilde{u}_x + \tilde{v}_y = 0$ and the kinematic viscosity are considered. This set of equations describes the physics of many phenomena in the engineering sciences, such as ocean currents, water flow in a pipe and air flow around a wing. It's well-known that the INS Eq. (1.1) admits an equivalent vorticity formulation, which can be written in the transport form:

$$\omega_t + \tilde{u}\omega_x + \tilde{v}\omega_y = \varepsilon \Delta \omega. \quad (1.2)$$

Here, ω is the vorticity, $\omega := \tilde{v}_x - \tilde{u}_y$, and therefore, Eq. (1.2) can be considered as a 2D viscous Hamilton-Jacobi (HJ) equation

$$\omega_t + H(\nabla \omega) = \varepsilon \Delta \omega, \quad (1.3)$$

with a global Hamiltonian $H(\nabla \omega) = \tilde{u}\omega_x + \tilde{v}\omega_y$.

In recent decades, successful activities to design, analyse and implement modern numerical schemes to approximate the solutions of HJ equations (1.3) have been performed by researchers, which can be referred to as [1, 5, 30, 32, 33] and [4]. Therefore, we are motivated to use existing ideas and apply them to numerically solve INS equations. Primary examples for these modern high-resolution schemes are upwind Godunov-type schemes. Osher et al. proposed high-order upwind schemes [21, 22] based on essentially non-oscillatory (ENO) reconstruction [11, 28, 29]. An adaptive-stencil selection approach is considered in the ENO reconstructions in order to eliminate or reduce spurious oscillation in non-smooth regions and to obtain maximum accuracy in smooth regions. Shu et al. modified the ENO reconstructions in [28, 29], which are more efficient for multi-dimensional cases. The first version of weighted ENO (WENO) schemes in framework of finite volume for 1D problems were constructed by Liu et al. [18]. The first version of WENO schemes

Received: 29 September 2021 ; Accepted: 30 March 2022.

* Corresponding author. Email: rabedian@ut.ac.ir.

in the context of finite difference, which is more efficient for multi-dimensional problems, was introduced by Jiang and Shu [15]. In 2000, authors of [14] proposed a fifth-order finite difference WENO scheme for solving HJ equations based on [15]. Weighted power ENO (WPENO) schemes with upwind fluxes for solving HJ equations were proposed by Serna and Qian [27] based on power ENO (PENO) schemes [26] for solving hyperbolic conservation laws. Combining ideas from PENO [26] and mapped WENO (MWENO) [13] reconstructions, Bryson and Levy proposed another algorithm for numerically solving HJ equations [9].

In this research work, we search to design a hybrid scheme for solving Eq. (1.3). This scheme uses a combination of a uniformly non-oscillatory (UNO) limiter and WENO reconstruction with the introduction of new non-linear weights. It should be noted that the combination of a UNO limiter and a third-order WENO reconstruction was first performed by Peer et al. [23] to solve the hyperbolic conservation laws. The numerical results in [23] illustrate that the use of limiters enhances the ENO reconstructions but in this idea, the existence of negative linear weights is avoidable, which should be solved. Abedian et al. [2] then proposed a new reconstruction to solve the hyperbolic conservation laws by combining a UNO limiter and a fifth-order WENO reconstruction with another idea to solve the problem of negative linear weights.

To design the new scheme, first, an optimum polynomial based on a three-point stencil is constructed. Next, the second-order ENO reconstruction by choosing an additional point inside the stencil is modified. Then, the optimum polynomial is rewritten as a convex combination of three polynomials with ideal weights. After that, following the methodology of the traditional WENO reconstruction, the new non-linear weights based on the linear weights are calculated.

The outline of this research is as follows. In section 2, the construction and implementation of the new scheme is described by detailing the INS equations. In section 3, several numerical experiments to demonstrate the accuracy and the resolution capability of the new scheme are prepared. Concluding remarks are given in section 4.

2. THE NUMERICAL SCHEME FOR INS EQUATIONS

In this section, first, the framework of the scheme will be given and then the detailed steps of the WHybUNO (weighted hybrid UNO) reconstruction will be presented.

2.1. 1D inviscid Hamilton-Jacobi equations. To begin, assume that the kinematic viscosity ε in Eq. (1.3) is equal to zero, so we have a inviscid Hamilton-Jacobi equations that in 1D case can be written as

$$\omega_t + H(\omega_x) = 0, \quad x \in \Omega = [a, b]. \quad (2.1)$$

A uniform mesh, defined as $a = x_0 < x_1 < \dots < x_{N-1} < x_N = b$, is considered. Also, $\omega_j = \omega(x_j, t)$ and $u_j = \omega_x(x_j, t)$ are denoted as the numerical approximation to the viscosity solution and its first derivative. Then the following ordinary differential equation (ODE) is obtained as:

$$\frac{d\omega_j}{dt} = -H(\omega_x)|_{x=x_j}. \quad (2.2)$$

Here, $H(\omega_x)|_{x=x_j}$ is replaced by a monotone numerical flux which is denoted by $\hat{H}(u_j^-, u_j^+)$ and the simple Lax-Friedrichs flux is used in this work. In the next subsection, the WHybUNO scheme will be described in detail which this scheme will be employed to approximate the left and right limits of the point values of $u(x_j, t)$ i.e. u_j^\pm . It should be noted that after the spatial discretization, the scheme can be rewritten as $\frac{dU}{dt} = F(U)$. Here, F denotes the operator of the spatial discretization. In this paper, the third-order total variation diminishing (TVD) Runge-Kutta time discretization [28] to solve the semi-discrete form Eq. (2.2) is employed.

2.2. WHybUNO reconstruction in one dimension. In this subsection, the WHybUNO reconstruction procedure for $u_j^\pm = \omega_{x,j}^\pm$ will be described.

Step 1. Given the big stencil $S = \{I_{j-1}, I_j, I_{j+1}\}$ and $S^0 = \{I_j, I_{j+1}\}$ and $S^1 = \{I_{j-1}, I_j\}$ where $I_j := [x_j - \Delta x, x_j]$, the polynomials $p_0(x)$, $p_1(x)$ and $p_2(x)$ are constructed as follows.



Let $U(x)$ be the primitive function of $u(x)$, $U(x) = \int_{-\infty}^x u(\xi)d\xi$, clearly

$$U(x_j) = \int_{-\infty}^{x_j} u(\xi)d\xi = \sum_{i=-\infty}^j \int_{x_{i-1}}^{x_i} u(\xi)d\xi = \sum_{i=-\infty}^j \Delta\omega_j, \tag{2.3}$$

where $\Delta\omega_j := \omega_j - \omega_{j-1}$. Now, we employ Newton’s interpolation formula to interpolate $U(x)$ at points $\{x_{j-2}, \dots, x_{j+1}\}$. If we show this interpolation polynomial with $P_2(x)$, then we have that

$$\tilde{p}_2(x) = P'_2(x) = \sum_{i=1}^3 U[x_{j-2}, \dots, x_{j+i-2}] \sum_{m=0}^{i-1} \prod_{l=0, l \neq m}^{i-1} (x - x_{j+l-2}), \tag{2.4}$$

where $U[\dots]$ is a divided difference of the function $U(x)$. In order to obtain a more efficient reconstruction, $\tilde{p}_2(x)$ is modified by interpolation over an additional point lying within the same stencil

$$p_2(x) = \tilde{p}_2(x) + U[x_{j-2}, \dots, x_{j+1}, x_{j-\frac{1}{2}}] \sum_{m=0}^3 \prod_{l=0, l \neq m}^3 (x - x_{j+l-2}). \tag{2.5}$$

Having obtained $p_2(x)$ as above, $p_r(x)$ from cell boundaries of the stencil S^r is obtained as

$$p_r(x) = \tilde{p}_r(x) + U[x_{j-r-1}, \dots, x_{j-r+1}, x_{j-\frac{1}{2}}] \sum_{m=0}^2 \prod_{l=0, l \neq m}^2 (x - x_{j-r+l-1}), \tag{2.6}$$

for $r = 0, 1$.

Remark 2.1. Firstly, we consider a general point as x_{j+ar+b} , and proceed with a Taylor series expansion to recognize the point which is giving the highest accuracy. Accordingly, we have $a = 0$ and $b = \frac{1}{2}$.

Remark 2.2. As can be seen, the polynomial $p_2(x)$ in Eq. (2.5), is of degree three, and thus the reconstruction (2.5) reproduce exactly polynomials of degree three on the stencil.

Remark 2.3. Polynomial (2.5) interpolates more points for later approximating the cell boundaries, and if the reconstruction is smooth (no discontinuities), we then obtain more accurate results. Hopefully, it also satisfies the conservation property.

Remark 2.4. The purpose of all polynomials of type (2.4) and (2.5) is to approximate the boundaries of cell I_j . By retaining more information within cell I_j , we intend to use data closer to the cell centre, rather than those further away.

In order to be able to obtain the polynomials $p_0(x), p_1(x)$ and $p_2(x)$ explicitly, a polynomial that retains information within the cell I_j is required. Similar to the NT scheme [20] proposed to improve the first-order Lax-Friedrichs scheme, the same polynomial is employed here,

$$L_j(x) = \frac{1}{\Delta x} (\Delta\omega_j + (x - x_{j-\frac{1}{2}})u'_j), \quad x \in I_j. \tag{2.7}$$

The divided differences $U[x_{j-r+1}, x_{j-\frac{1}{2}}]$ for $r = 0, 1$ are given by

$$\begin{aligned} U[x_{j-r+1}, x_{j-\frac{1}{2}}] &= \frac{1}{x_{j-\frac{1}{2}} - x_{j-r+1}} \int_{x_{j-r+1}}^{x_{j-\frac{1}{2}}} \left(\sum_j L_j(x) \chi_j(x) \right) dx \\ &= \frac{1}{12} \left((1 + 2r) \left(4 \frac{\Delta\omega_j}{\Delta x} + u'_j \right) + 8(1 - r) \frac{\Delta\omega_{j+1}}{\Delta x} \right), \end{aligned} \tag{2.8}$$

where $\chi_j(x)$ is the characteristic function of the cell I_j . The numerical derivative u'_j , is approximated by the UNO limiter [12]:

$$u'_j = \frac{1}{\Delta x} \text{MM} \left(a_j + \frac{1}{2} \text{MM}(b_{j-1}, b_j), a_{j+1} - \frac{1}{2} \text{MM}(b_j, b_{j+1}) \right), \tag{2.9}$$



where $a_j := \Delta\omega_j - \Delta\omega_{j-1}$, $b_j := \Delta\omega_{j+1} - 2\Delta\omega_j + \Delta\omega_{j-1}$ and the definition of the **MM** function is:

$$\begin{aligned} \text{MM}(x_1, \dots, x_m) &= \begin{cases} k \min_{1 \leq p \leq m} \{|x_p|\} & \text{if } k = \text{sign}(x_1) = \dots = \text{sign}(x_m), \\ 0 & \text{otherwise.} \end{cases} \end{aligned} \quad (2.10)$$

Step 2. The smoothness indicators for each stencil are computed. They measure the smoothness of the functions in each stencil: the smaller the indicator is, the smoother the function is in the stencil. The smoothness indicator of each function, demonstrated by β_i , is explicitly calculated by the following formula:

$$\beta_i = \sum_{k=1}^2 \Delta x^{2k-1} \int_{I_j} \left(\frac{d^k}{dx^k} p_i(x) \right)^2 dx, \quad i \in \{0, 1, 2\}. \quad (2.11)$$

A direct computation based on (2.5), and (2.6) yields:

$$\begin{aligned} \beta_0 &= \frac{13}{3} \left(\frac{a_{j+1}}{\Delta x} - u'_j \right)^2 + (u'_j)^2, & \beta_1 &= \frac{13}{3} \left(\frac{a_j}{\Delta x} - u'_j \right)^2 + (u'_j)^2, \\ \beta_2 &= \frac{9}{2916} \left(\frac{\Delta\omega_{j-1}}{\Delta x} - \frac{\Delta\omega_{j+1}}{\Delta x} - 16u'_j \right)^2 + \frac{13}{12} \left(\frac{b_j}{\Delta x} \right)^2 + \frac{449856}{58320} \left(\frac{\Delta\omega_{j-1}}{\Delta x} - \frac{\Delta\omega_{j+1}}{\Delta x} + 2u'_j \right)^2. \end{aligned} \quad (2.12)$$

Step 3. The non-linear weights w_j are computed by

$$w_j = \frac{\bar{w}_j}{\sum_k \bar{w}_k}, \quad \bar{w}_k = \gamma_k \left(1 + \frac{\tau}{\epsilon + \beta_k} \right), \quad j, k = 0, 1, 2, \quad (2.13)$$

where γ_k are the linear weights and $\epsilon = 10^{-40}$ is considered to avoid the denominator to be zero. Here, τ is a global smoothness indicator which in this paper, we propose a new global smooth indicator as:

$$\tau = \left| \frac{\beta_0 + \beta_1}{2} - \beta_2 \right|. \quad (2.14)$$

Step 4. The final WHyBENO reconstruction is given by

$$R(x) = w_2 \left(\frac{1}{\gamma_2} p_2(x) - \frac{\gamma_0}{\gamma_2} p_0(x) - \frac{\gamma_1}{\gamma_2} p_1(x) \right) + w_1 p_1(x) + w_0 p_0(x). \quad (2.15)$$

The right side of Eq. (2.15) is different from the traditional WHyBENO [2, 3, 23] schemes. Reconstruction (2.15) clearly allows the linear weights to be arbitrary provided $\gamma_0 + \gamma_1 + \gamma_2 = 1$. Accordingly,

$$u_j^- = R(x_j), \quad u_{j-1}^+ = R(x_{j-1}).$$

Remark. For the two-dimensional problems, all of these reconstruction steps are performed in a dimension-by-dimension fashion.

2.3. 2D viscous Hamilton-Jacobi equations. Consider Eq. (1.3). Let (x_j, y_k) be a discretization of $\Omega \subseteq \mathbb{R}^2$ with uniform spacing Δx and Δy . Also, denoting $\omega(x_j, y_k)$, $\omega_x(x_j, y_k)$ and $\omega_y(x_j, y_k)$ by $\omega_{j,k}$, $u_{j,k}$ and $v_{j,k}$, respectively. Then the following ODE is obtained as:

$$\frac{d\omega_{j,k}}{dt} = -\hat{H}(u_{j,k}^-, u_{j,k}^+, v_{j,k}^-, v_{j,k}^+) + \varepsilon(\Delta\omega)|_{x=x_j, y=y_k}, \quad (2.16)$$

where, $\hat{H}(u_{j,k}^-, u_{j,k}^+, v_{j,k}^-, v_{j,k}^+)$ is the simple Lax-Friedrichs flux. To approximate $(\Delta\omega)|_{x=x_j, y=y_k}$ by $\Delta\omega_{j,k}$, the fourth-order central differencing is employed as:

$$\Delta\omega_{j,k} = \frac{-w_{j+2,k} + 16w_{j+1,k} - 30w_{j,k} + 16w_{j-1,k} - w_{j-2,k}}{12\Delta x^2} + \frac{-w_{j,k+2} + 16w_{j,k+1} - 30w_{j,k} + 16w_{j,k-1} - w_{j,k-2}}{12\Delta y^2}. \quad (2.17)$$

Since the Hamiltonian ($H(w_x, w_y) = \tilde{u}w_x + \tilde{v}w_y$) is global, the implementation of WHyBENO requires the velocities $\{\tilde{u}_{j,k}, \tilde{v}_{j,k}\}$ to be recovered from the known values of the vorticity $\{\omega_{j,k}\}$ at each time level. This issue can be solved with the help of the stream function ψ , such that $\tilde{u} = \psi_y$, $\tilde{v} = -\psi_x$ and $\Delta\psi = -\omega$. As can be seen, we are faced with



TABLE 1. Errors and orders of convergence for Example 3.1 at T=2

$N_x \times N_y$	L_1 error	L_1 order	L_∞ error	L_∞ order
WENO3-JP scheme				
20 × 20	1.47(-1)	-	2.15(-1)	-
40 × 40	5.33(-2)	1.46	9.47(-2)	1.18
80 × 80	1.47(-2)	1.86	3.73(-2)	1.34
160 × 160	1.84(-3)	2.99	8.30(-3)	2.17
320 × 320	2.06(-4)	3.16	1.44(-3)	2.53
WHybUNO(1) scheme				
20 × 20	2.54(-2)	-	8.72(-2)	-
40 × 40	3.96(-3)	2.69	1.25(-2)	2.80
80 × 80	5.38(-4)	2.88	1.48(-3)	3.08
160 × 160	5.87(-5)	3.19	1.80(-4)	3.04
320 × 320	9.64(-6)	2.61	2.58(-5)	2.80
WHybUNO(2) scheme				
20 × 20	3.08(-2)	-	8.72(-2)	-
40 × 40	4.07(-3)	2.92	1.15(-2)	2.92
80 × 80	5.38(-4)	2.93	1.48(-3)	2.96
160 × 160	6.73(-5)	3.00	1.80(-4)	3.03
320 × 320	8.41(-6)	3.00	2.31(-5)	2.96
WHybUNO(3) scheme				
20 × 20	2.55(-2)	-	8.96(-2)	-
40 × 40	3.36(-3)	2.92	1.12(-3)	3.00
80 × 80	4.82(-4)	2.80	1.61(-3)	2.80
160 × 160	5.55(-5)	3.12	1.85(-4)	3.12
320 × 320	7.96(-6)	2.80	2.13(-5)	3.12

a Poisson equation at each time level that can be solved using the FFT based pseudo-spectral technique. Thus, the velocities via the fourth-order finite differences of the stream function are computed as:

$$\begin{aligned} \tilde{u}_{j,k} &= \frac{-\psi_{j,k+2} + 8\psi_{j,k+1} - 8\psi_{j,k-1} + \psi_{j,k-2}}{12\Delta y}, \\ \tilde{v}_{j,k} &= \frac{\psi_{j+2,k} - 8\psi_{j+1,k} + 8\psi_{j-1,k} - \psi_{j-2,k}}{12\Delta x}. \end{aligned} \tag{2.18}$$

3. COMPUTATIONAL RESULTS

In this section, the numerical performance of WHybUNO scheme is compared with the classical third-order WENO [14], named as WENO3-JP. To test the claim that linear weights in WHybUNO scheme can be arbitrarily selected, the following types of linear weights are first considered: (1) $\gamma_0 = \gamma_1 = 0.01, \gamma_2 = 0.98$; (2) $\gamma_0 = \gamma_1 = \gamma_2 = \frac{1}{3}$; (3) $\gamma_0 = \gamma_1 = 0.495, \gamma_2 = 0.01$.

Example 3.1. In this example, the accuracy of the WHybUNO scheme for Eq. (1.3) with $\varepsilon = 0.01$ and periodic boundary conditions in $[0, 2\pi] \times [0, 2\pi]$ is tested [31]. The initial condition is $\omega(x, y, 0) = -2 \sin(x) \sin(y)$. The exact solution is $\omega(x, y, t) = -2 \sin(x) \sin(y) \exp(-2\varepsilon t)$. The errors and numerical orders of accuracy at $T = 2$ are reported in Table 1. The WHybUNO scheme achieves its designed order of accuracy and generates less absolute errors. Table 1 also presents the results of the WHybUNO scheme with different types of linear weights. As can be seen, WHybUNO scheme with different types of linear weights has also been able to achieve third-order accuracy.



TABLE 2. Errors and orders of convergence for Example 3.2 at T=4

$N_x \times N_y$	L_1 error	L_1 order	L_∞ error	L_∞ order
WENO3-JP scheme				
20×20	3.17(-1)	-	3.24(-1)	-
40×40	1.08(-1)	1.56	1.55(-1)	1.06
80×80	3.49(-2)	1.62	6.34(-2)	1.29
160×160	9.21(-3)	1.92	2.31(-2)	1.46
320×320	1.80(-3)	2.35	8.59(-3)	1.43
WHybUNO(1) scheme				
20×20	1.48(-1)	-	1.91(-1)	-
40×40	2.20(-2)	2.75	3.41(-2)	2.49
80×80	3.27(-3)	2.75	4.62(-3)	2.88
160×160	3.95(-4)	3.05	5.84(-4)	2.98
320×320	4.56(-5)	3.12	7.05(-5)	3.05
WHybUNO(2) scheme				
20×20	1.35(-1)	-	2.00(-1)	-
40×40	2.06(-2)	2.72	3.57(-2)	2.49
80×80	2.92(-3)	2.82	4.89(-3)	2.87
160×160	3.69(-4)	2.98	6.12(-4)	3.00
320×320	4.25(-5)	3.12	7.56(-5)	3.02
WHybUNO(3) scheme				
20×20	1.52(-1)	-	1.89(-1)	-
40×40	2.31(-2)	2.72	3.26(-2)	2.54
80×80	3.59(-3)	2.69	4.31(-3)	2.92
160×160	4.23(-4)	3.08	5.45(-4)	2.98
320×320	5.00(-5)	3.08	6.74(-5)	3.01

Example 3.2. Now, the Burgers vortex problem is considered. It is a steady viscous vortex maintained by a secondary flow. The corresponding equation is

$$\omega_t + (-\alpha_0 x + u)\omega_x + (-\alpha_1 y + v)\omega_y = (\alpha_0 + \alpha_1)\omega + \varepsilon\Delta\omega. \quad (3.1)$$

When $\alpha_0 = \alpha_1 > 0$, $\omega(x, y) = A \exp\left(-\frac{\alpha_0(x^2 + y^2)}{2\varepsilon}\right)$ is an exact steady solution [24]. For parameters in this problem, the constants $A = 10$, $\alpha_0 = 0.012$ and $\varepsilon = 0.0025$ are chosen. The errors and numerical orders of accuracy at $T = 4$ for the computing domain $[-3.5, 3.5] \times [-3.5, 3.5]$ are reported in Table 2. Table 2 also demonstrates the errors and convergence orders of WHybUNO scheme with different types of linear weights. The WHybUNO scheme achieves its designed order of accuracy and generates less absolute errors.

Example 3.3. In this example, the Lamb-Oseen vortex problem is considered [25]. This problem models a line vortex that decays due to viscosity and it is named after Horace Lamb and Carl Wilhelm Oseen. Eq. (1.3) in the computing domain $[-2\pi, 2\pi] \times [-2\pi, 2\pi]$ with $\varepsilon = 0.00037$ is solved. The initial condition in this problem is $\omega(x, y, 0) = 2\pi \exp(-(x^2 + y^2))$ and the exact solution is $\omega(x, y, t) = \frac{2\pi}{1+4\varepsilon t} \exp\left(-\frac{x^2 + y^2}{1+4\varepsilon t}\right)$. In Table 3, the errors and numerical orders of accuracy at $T = 4$ are listed. This table also reports the errors and numerical convergence orders of WHybUNO scheme with different types of linear weights. As can be seen, the WHybUNO method attains its designed order of accuracy and generates less absolute errors.



TABLE 3. Errors and orders of convergence for Example 3.3 at T=4

$N_x \times N_y$	L_1 error	L_1 order	L_∞ error	L_∞ order
WENO3-JP scheme				
20 × 20	6.11(-1)	-	5.31(-1)	-
40 × 40	2.18(-1)	1.49	2.13(-1)	1.32
80 × 80	6.62(-2)	1.72	8.56(-2)	1.32
160 × 160	1.62(-2)	2.03	2.53(-2)	1.76
320 × 320	2.33(-3)	2.80	6.69(-3)	1.92
WHybUNO(1) scheme				
20 × 20	8.56(-2)	-	6.32(-2)	-
40 × 40	1.06(-2)	3.00	8.25(-3)	2.94
80 × 80	1.39(-3)	2.94	9.37(-4)	3.13
160 × 160	1.74(-4)	3.01	1.19(-4)	2.97
320 × 320	2.11(-5)	3.03	1.60(-5)	2.90
WHybUNO(2) scheme				
20 × 20	8.56(-2)	-	6.32(-2)	-
40 × 40	1.17(-2)	2.87	8.85(-3)	2.84
80 × 80	1.46(-3)	3.00	1.08(-3)	3.04
160 × 160	1.78(-4)	3.04	1.41(-4)	2.94
320 × 320	2.16(-5)	3.04	1.67(-5)	3.07
WHybUNO(3) scheme				
20 × 20	9.63(-2)	-	7.45(-2)	-
40 × 40	1.23(-2)	2.97	9.95(-3)	2.90
80 × 80	1.53(-3)	3.00	1.27(-3)	2.97
160 × 160	1.91(-4)	3.00	1.51(-4)	3.07
320 × 320	2.38(-5)	3.00	1.75(-5)	3.11

Example 3.4. In this example, the vortex patch problem is considered [31]. Thus, the INS equation (1.3) with $\varepsilon = 0.01$ in the computing domain $[0, 2\pi] \times [0, 2\pi]$ is solved. the initial condition is

$$\omega(x, y, 0) = \begin{cases} -1, & (x, y) \in [\frac{\pi}{2}, \frac{3\pi}{2}] \times [\frac{\pi}{4}, \frac{3\pi}{4}], \\ 1, & (x, y) \in [\frac{\pi}{2}, \frac{3\pi}{2}] \times [\frac{5\pi}{4}, \frac{7\pi}{4}], \\ 0, & \text{otherwise,} \end{cases} \tag{3.2}$$

while the periodic boundary conditions are assigned. The data at $T = 1$ and $T = 5$ is recorded with $N_x \times N_y = 64 \times 64$ sub-equal intervals and the numerical solution of WHybUNO(1) is presented in Figure 1. The results compare well with those reported in [31].

Example 3.5. In this example, a study of the axisymmetrization of an isolated vortex will be conducted. This problem was first proposed by Melander, McWilliams and Zabusky in 1987 [19] and in this paper it is named as MMZ vortex. Therefore, Eq. (1.3) with the following initial condition:

$$\omega(x, y, 0) = \begin{cases} 20 - 20 \exp(-\frac{\kappa}{r} \exp(\frac{1}{r-1})), & r < 1, \\ 0, & r \geq 0, \end{cases} \tag{3.3}$$

where $r = \sqrt{\frac{x^2}{2} + 2y^2}$ and $\kappa = \frac{1}{2}e^2 \ln(2)$ is solved. Eq. (3.3) is an elliptical vortex with a smooth transition between irrotational and rotational fluid. The computing domain for simulations is $[-\pi, \pi] \times [-\pi, \pi]$ and we test this problem with two different viscosity, $\varepsilon = 10^{-7}$ and $\varepsilon = 3.125 \times 10^{-8}$. The obtained results by WHybUNO(1) scheme with



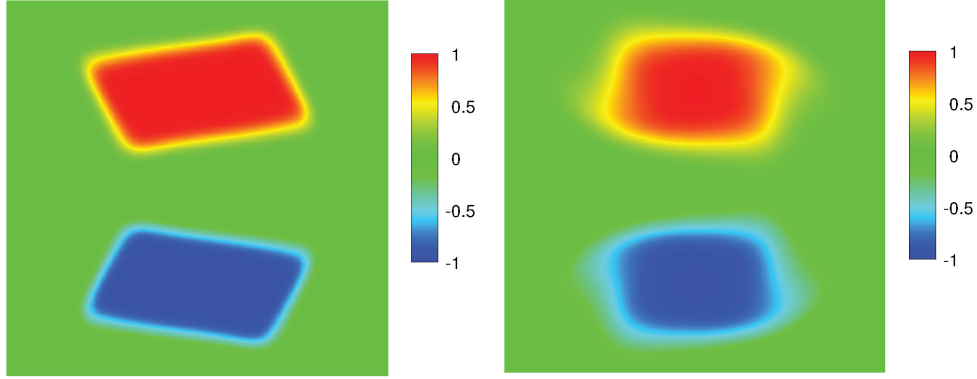


FIGURE 1. The vortex patch problem in the computing domain $[0, 2\pi] \times [0, 2\pi]$, left: $T = 1$ and right: $T = 5$.

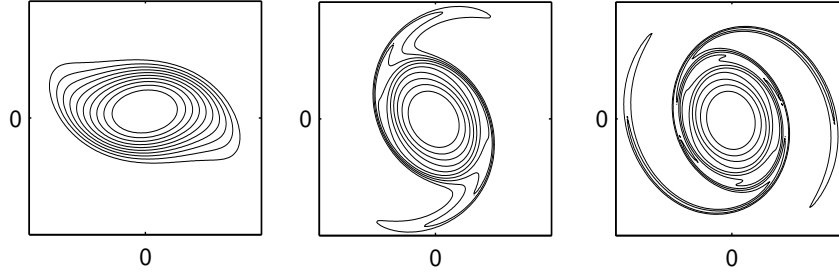


FIGURE 2. The MMZ vortex problem in the computing domain $[-\pi, \pi] \times [-\pi, \pi]$ with $\nu = 10^{-7}$, left: $T = 0.25$; middle: $T = 0.9$ and right: $T = 1.65$. (Only the box $[-2.2, 2.2] \times [-2.2, 2.2]$ in which the vortex is non-zero is displayed.)

$N_x \times N_y = 128 \times 128$ sub-equal intervals at different final times for $\varepsilon = 10^{-7}$ are demonstrated in Figure 2. The results agree well with the results given in [6, 19]. Now, the WhybUNO(1) scheme is employed to obtain solution of the MMZ vortex problem at different times with $N_x \times N_y = 128 \times 128$ sub-equal intervals and $\varepsilon = 3.125 \times 10^{-8}$. The results are demonstrated in Figure 3. Again, the results agree well with the results given in [16].

Example 3.6. As the last example, consider the double shear-layer model problem. This problem was first proposed by Bell, Colella and Glaz in 1989 [7] and see [8, 17] for more details on this problem. Accordingly, Eq. (1.3) with initial condition

$$\tilde{u}(x, y, 0) = \begin{cases} \tanh\left(\frac{1}{\rho}\left(y - \frac{\pi}{2}\right)\right), & y \leq \pi, \\ \tanh\left(\frac{1}{\rho}\left(\frac{3\pi}{2} - y\right)\right), & y > \pi, \end{cases} \quad \tilde{v}(x, y, 0) = \delta \cdot \sin x, \quad (3.4)$$

where $\rho = \frac{\pi}{15}$ and $\delta = 0.05$ in the computing domain $[0, 2\pi] \times [0, 2\pi]$ is solved. The final time of this problem is $T = 10$. The WhybUNO(1) scheme is used to obtain the vorticity of the double shear-layer model problem with $N_x \times N_y = 256 \times 256$ sub-equal intervals. Figure 4 demonstrates the vorticity for $\varepsilon = 0$ and $\varepsilon = 5 \times 10^{-4}$ and as can be seen WhybUNO scheme generates a super resolution without any spurious oscillations typically appearing near the stagnation point. Also, the results compare well with those reported in [10].



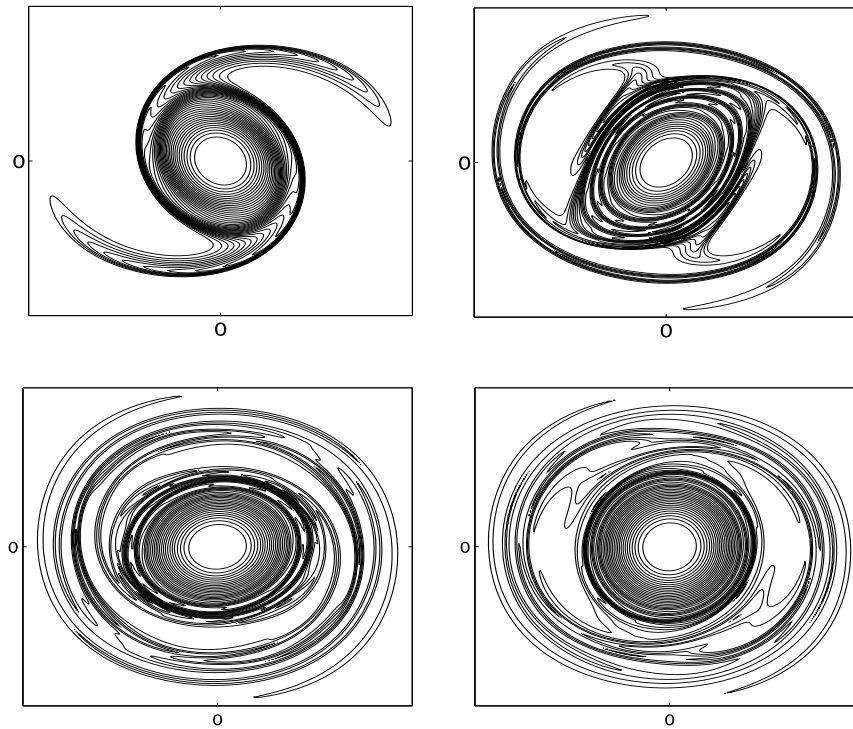


FIGURE 3. The MMZ vortex problem in the computing domain $[-\pi, \pi] \times [-\pi, \pi]$ with $\nu = 3.125 \times 10^{-8}$, top(left): $T = 1$; top(right): $T = 4$; bottom(left): $T = 8$ and bottom(right): $T = 10$. (Only the box $[-2.2, 2.2] \times [-2.2, 2.2]$ in which the vortex is non-zero is displayed.)

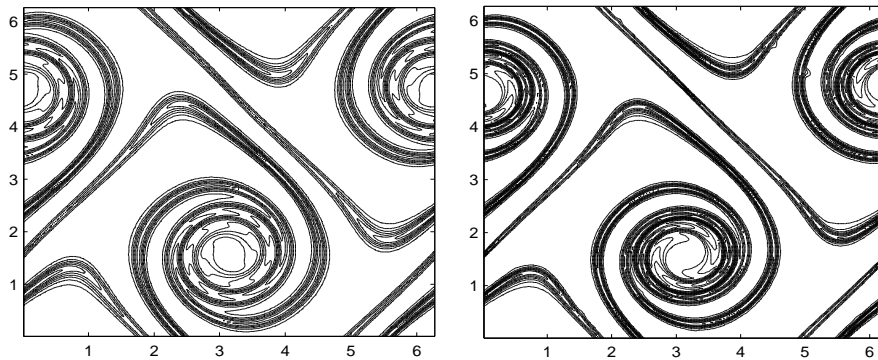


FIGURE 4. The double shear-layer model problem in the computing domain $[0, 2\pi] \times [0, 2\pi]$ at the final time $T = 10$. Left: $\varepsilon = 5 \times 10^{-4}$ and right: $\varepsilon = 0$.

4. CONCLUDING REMARKS

In this work, a new weighted hybrid ENO (WHybUNO scheme) reconstruction for solving 2D incompressible Navier-Stokes equations is designed. This new reconstruction results from a non-linear convex combination of three polynomials. It is explored that this reconstruction generates a third-order scheme in smooth regions and maintains



non-oscillatory properties for problems with strong shocks. As the next research work, this scheme will be developed to track the Oseen vortex as a maximum entropy state of a 2D flow. The WHybUNO schemes may also be employed in tracking the phenomena of thermocapillary drop migration, where velocity far away from the drop is almost zero.

ACKNOWLEDGEMENTS

The author is very thankful to the reviewers for carefully reading the paper, their comments and suggestions have improved the quality of the paper.

REFERENCES

- [1] R. Abedian, *A symmetrical WENO-Z scheme for solving Hamilton-Jacobi equations*, Int. J. Mod. Phys. C, *31* (2020), 2050039.
- [2] R. Abedian, H. Adibi, and M. Dehghan, *A high-order symmetrical weighted hybrid ENO-flux limiter scheme for hyperbolic conservation laws*, Comput. Phys. Commun., *185* (2014), 106–127.
- [3] R. Abedian, H. Adibi, and M. Dehghan, *Symmetrical weighted essentially non-oscillatory-flux limiter schemes for Hamilton-Jacobi equations*, Math. Methods Appl. Sci., *38* (2015), 4710–4728.
- [4] R. Abedian and M. Dehghan, *RBF-ENO/WENO schemes with Lax-Wendroff type time discretizations for Hamilton-Jacobi equations*, Numer. Methods Partial Differ. Equ., *37* (2021), 594–613.
- [5] R. Abedian and R. Salehi, *A RBFWENO finite difference scheme for Hamilton-Jacobi equations*, Comput. Math. with Appl., *79* (2020), 2002–2020.
- [6] L. A. Barba and L. F. Rossi, *Global field interpolation for particle methods*, J. Comput. Phys., *229*, 1292–1310.
- [7] J. B. Bell, P. Colella, and H. M. Glaz, *A second-order projection method for the incompressible Navier-Stokes equations*, J. Comput. Phys., *85* (1989), 257–283.
- [8] D. L. Brown and M. L. Minion, *Performance of under-resolved two-dimensional incompressible flow simulations*, J. Comput. Phys., *122* (1995), 165–183.
- [9] S. Bryson and D. Levy, *Mapped WENO and weighted power ENO reconstructions in semi-discrete central schemes for Hamilton-Jacobi equations*, Appl. Numer. Math., *56* (2006), 1211–1224.
- [10] A. Chertock and A. Kurganov, *On Splitting-Based Numerical Methods for Convection-Diffusion Equations*, Quad. Mat., *24* (2009), 303–343.
- [11] A. Harten, B. Engquist, S. Osher, and S. Chakravarthy, *Uniformly high-order essentially non-oscillatory schemes, III*, J. Comput. Phys., *71* (1987), 231–303.
- [12] A. Harten and S. Osher, *Uniformly high-order accurate nonoscillatory schemes I*, SIAM J. Numer. Anal., *24* (1987), 279–309.
- [13] A. K. Henrick, T. D. Aslam, and J. M. Powers, *Mapped weighted essentially non-oscillatory schemes: Achieving optimal order near critical points*, J. Comput. Phys., *207* (2005), 542–567.
- [14] G.-S. Jiang and D. Peng, *Weighted ENO schemes for Hamilton-Jacobi equations*, SIAM J. Sci. Comput., *21* (2000), 2126–2143.
- [15] G.-S. Jiang and C.-W. Shu, *Efficient implementation of weighted ENO schemes*, J. Comput. Phys., *126* (1996), 202–228.
- [16] P. Koumoutsakos, *Inviscid axisymmetrization of an elliptical vortex*, J. Comput. Phys., *138* (1997), 821–857.
- [17] A. Kurganov, S. Noelle, and G. Petrova, *Semi-discrete central-upwind schemes for hyperbolic conservation laws and Hamilton-Jacobi equations.*, SIAM J. Sci. Comput., *23* (2001), 707–740.
- [18] X.-D. Liu, S. Osher, and T. Chan, *Weighted essentially non-oscillatory schemes*, J. Comput. Phys., *115* (1994), 200–212.
- [19] M. Melander, J. McWilliams, and N. Zabusky, *Axisymmetrization and vorticity-gradient intensification of an isolated two-dimensional vortex through filamentation*, J. Fluid Mech., *178* (1987), 137–159.
- [20] H. Nessyahu and E. Tadmor, *Non-oscillatory central differencing for hyperbolic conservation laws*, J. Comput. Phys., *87* (1990), 408–463.
- [21] S. Osher and J. Sethian, *Fronts propagating with curvature dependent speed: algorithms based on Hamilton-Jacobi formulations*, J. Comput. Phys., *79* (1988), 12–49.



- [22] S. Osher and C.-W. Shu, *High-order essentially nonoscillatory schemes for Hamilton-Jacobi equations*, SIAM J. Numer. Anal., *28* (1991), 907–922.
- [23] A. A. I. Peer, M. Z. Dauhoo, A. Gopaul, and M. Bhuruth, *A weighted ENO-flux limiter scheme for hyperbolic conservation laws*, Int. J. Comput. Math, *87* (2010), 3467–3488.
- [24] A. Robinson and P. Saffman, *Stability and structure of stretched vortices*, Stud. Appl. Math., *70* (1984), 163–181.
- [25] P. Saffman, M. Ablowitz, E. Hinch, J. Ockendon, and P. Olver, *Vortex dynamics*, Cambridge University Press, Cambridge, 1992.
- [26] S. Serna and A. Marquina, *Power ENO methods: a fifth-order accurate weighted power ENO method*, J. Comput. Phys., *194* (2004), 632–658.
- [27] S. Serna and J. Qian, *Fifth order weighted power-ENO methods for Hamilton-Jacobi equations*, J. Sci. Comput., *29* (2006), 57–81.
- [28] C.-W. Shu and S. Osher, *Efficient implementation of essentially non-oscillatory shock-capturing schemes*, J. Comput. Phys., *77* (1988), 439–471.
- [29] C.-W. Shu and S. Osher, *Efficient implementation of essentially non-oscillatory shock-capturing schemes II*, J. Comput. Phys., *83* (1989), 32–78.
- [30] Z. Tao and J. Qiu, *Dimension-by-dimension moment-based central Hermite WENO schemes for directly solving Hamilton-Jacobi equations*, Adv. Comput. Math., *43* (2017), 1023–1058.
- [31] T. Xiong, G. Russo, and J.-M. Qiu, *High order multi-dimensional characteristics tracing for the incompressible Euler equation and the guiding-center Vlasov equation*, J. Sci. Comput., *77* (2018), 263–282.
- [32] F. Zheng, C.-W. Shu, and J. Qiu, *Finite difference Hermite WENO schemes for the Hamilton-Jacobi equations*, J. Comput. Phys., *337* (2017), 27–41.
- [33] J. Zhu and J. Qiu, *A new fifth order finite difference WENO scheme for Hamilton-Jacobi equations*, Numer. Methods Partial Differ. Equ., *33* (2017), 1095–1113.

